The acquisition of multidimensional NMR spectra within a single scan

Lucio Frydman[†‡], Tali Scherf[§], and Adonis Lupulescu[†]

Departments of [†]Chemical Physics and [§]Chemical Services, Weizmann Institute of Science, 76100 Rehovot, Israel

Communicated by Alexander Pines, University of California, Berkeley, CA, October 23, 2002 (received for review August 6, 2002)

A scheme enabling the complete sampling of multidimensional NMR domains within a single continuous acquisition is introduced and exemplified. Provided that an analyte's signal is sufficiently strong, the acquisition time of multidimensional NMR experiments can thus be shortened by orders of magnitude. This could enable the characterization of transient events such as proteins folding, 2D NMR experiments on samples being chromatographed, bring the duration of higher dimensional experiments (e.g., 4D NMR) into the lifetime of most proteins under physiological conditions, and facilitate the incorporation of spectroscopic 2D sequences into *in vivo* imaging investigations. The protocol is compatible with existing multidimensional pulse sequences and can be implemented by using conventional hardware; its performance is exemplified here with a variety of homonuclear 2D NMR acquisitions.

Few analytical techniques in science match in either breadth or depth the impact achieved by nuclear magnetic resonance (NMR) (1). After establishing itself as a tool for the characterization of organic molecules (2), the use of NMR has spread throughout the decades, reaching into areas as diverse as pharmaceutics, metabolic studies, structural biology, solid state chemistry, condensed matter physics, rheology, medical diagnosis (where it is known as MRI), and more recently neurobiology (1–8). In addition to assuming in all these disciplines a position of preeminence, the principles of NMR have served as paradigm to other physical methods that also rely on the interaction between radiation and matter (9, 10). Lying at the core of the expansion of NMR are powerful protocols developed over the years for characterizing the nuclear spin environment; in particular, the Fourier transform (FT) and the multidimensional method of NMR analysis (11–13). Contemporary NMR applications in all the scientific disciplines mentioned above rely routinely on Fourier and multidimensional spectroscopies for their implementation.

Unidimensional Fourier spectroscopy brings the so-called multiplex advantage into NMR, enabling a shortening in the data-scanning time by orders of magnitude and bringing about a concomitant increase in the signal-to-noise ratio (S/N) achievable per unit time. FT-NMR methods, the principles of which eventually extended to many other forms of spectroscopy (14), encode the complete spectral distribution $I(\nu)$ being sought by acquiring a single time-domain transient $S(t)$, from which $I(\nu)$ is reconstructed via a discrete version of the FT calculation $I(\nu) = (1/2\pi)\int_0^{AT} S(t)e^{-i\nu t}dt$. By contrast, the goal of multidimensional spectroscopy is not just to measure but to correlate NMR frequencies over several spectral dimensions. For instance in 2D NMR, the scheme (13)

$$\text{preparation} - \text{evolution}\ (t_1) - \text{mixing} - \text{acquistion}\ (t_2) \qquad \textbf{[1]}$$

provides a time-domain set $S(t_1, t_2)$, from which correlations between frequencies during the evolution and acquisition periods can be extracted as $I(\nu_1,\nu_2) = \int_0^{AT_1}\int_0^{AT_2} S(t_1, t_2)e^{-i\nu_1 t_1}e^{-i\nu_2 t_2}dt_1dt_2$. Collecting the 2D $S(t_1, t_2)$ NMR data set over sufficiently large regions of the time domain is usually carried out by a parametric increment of t_1 in N_1 steps of duration Δt_1, followed by a conventional t_2 acquisition in dwell times Δt_2. The extent of the sampling along the t_1 and t_2 domains eventually determines the line shapes of the final 2D NMR peaks: their so-called point-spread functions. Obtaining purely absorptive 2D NMR line shapes usually demands the collection of complementary data sets consisting of several N_1 points (15, 16); because each of these points constitutes an independent signal acquisition, 2D NMR relinquishes to some extent the original ability of 1D FT NMR to retrieve a complete spectrum within a single scan. Indeed even in cases where the S/N is outstanding, 2D NMR experiments still may demand the acquisition of hundreds of transients to sample the t_1 domain adequately; this complication is compounded further in higher dimensional NMR.

The relatively slow multiscan approach of multidimensional FT spectroscopy was found particularly confining in 2D MRI. Yet in this case the availability of intense signals combined with an unparalleled flexibility available for manipulating the MRI interactions enabled the eventual development of ultrafast multidimensional acquisition techniques (ref. 17 and references therein). Principal among these techniques is echo planar imaging (EPI), which fully expands the multiplex advantage of FT NMR into several dimensions (18). Only rarely, however, could the principles underlying EPI be exported directly into high-resolution NMR spectroscopy (19–21). The purpose of the present article is to introduce an alternative that bypasses this limitation; a general Fourier-based scheme, the potential of which we exemplify in Fig. 1 with the high-resolution 2D NMR total correlation spectroscopy (TOCSY) spectrum of a peptide collected in a fraction of a second.

Methods

The general scheme for the experiment that we propose follows the canonical multidimensional spectroscopy outline given in Eq. **1** for the case of 2D NMR. By contrast to Eq. **1**, however, our proposal does not involve a homogeneous initial excitation of all spins but a heterogeneous one, with the selectivity being achieved via the introduction of an inhomogeneous spectral distribution within the sample.[¶] Once this artificial spectral heterogeneity has been imposed, the sample can be viewed as composed of independent subensembles, the evolution of which can be manipulated selectively. Selective manipulations can in turn be used toward the complete multiplexing of multidimensional NMR acquisitions, if exploited as illustrated in Fig. 2. Such a scheme assumes a single-axis B_o field gradient that is the source of spectral heterogeneities and a generic 2D NMR sequence that we summarize as

Abbreviations: FT, Fourier transform; S/N, signal-to-noise ratio; EPI, echo planar imaging; TOCSY, total correlation spectroscopy.

[‡]To whom correspondence should be addressed. E-mail: lucio.frydman@weizmann.ac.il.

[¶]In the case of NMR of liquids, this heterogeneity can be achieved via the application of external magnetic field gradients discriminating spins according to their position; for solids, the intrinsic anisotropy of the spin interactions could be exploited for achieving a similar orientation-dependent discrimination.

www.pnas.org/cgi/doi/10.1073/pnas.252644399

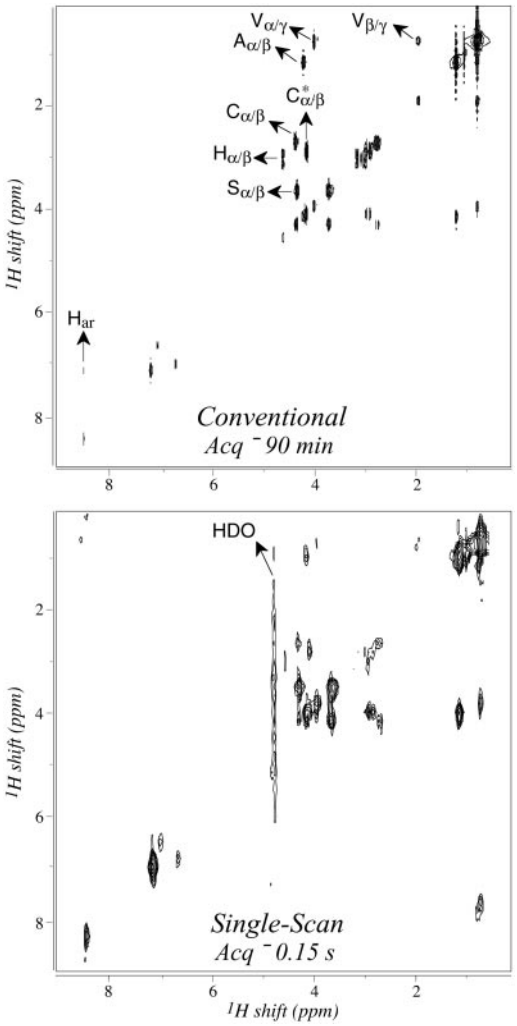

Fig. 1. Comparison between 2D magnitude TOCSY ^{1}H NMR spectra obtained by using the single-scan protocol introduced in the present study, *vis-à-vis* its conventional counterpart (22). Both spectra were collected on ≈15 mg of a hexapeptide (CSHAVC*) dissolved in ^2H_2O and show similar intraresidue cross-peak connectivities (tentatively assigned by the arrows). The single-scan data collection involved 61 × 256 points; the conventional 2D NMR spectrum collected a 128 × 2,048 (t_1,t_2) data matrix by using a phase cycle with 16 scans per t_1 point and 8 dummy scans. Both data sets were collected on a Bruker DMX500 NMR spectrometer by using a Nalorac Z-Spec TXI probehead. Further experimental details on the single-scan protocol are discussed in the text.

$$\left[\begin{array}{c}\text{slice-selective}\\ \text{preparation}\end{array}\right]_{N_1} \_\ \begin{array}{c}\text{position-dependent}\\ \text{evolution } (t_1)\end{array}$$

$$\_\ \begin{array}{c}\text{position-independent}\\ \text{mixing}\end{array} \_\ \begin{array}{c}\text{spatially decoded}\\ \text{acquisition } (t_2)\end{array} . \qquad [2]$$

An important difference between this scheme and Eq. **1** is that spins here are excited not with a single but with a train of consecutive pulses, each spectrally selective. As a result the sample is effectively partitioned into N_1 subensembles, each characterized by an individual t_1 evolution time. For the purpose of Fourier processing, it is convenient to space out the resulting train of slice-selective excitation pulses in constant intervals Δt_1 and then conclude the N_1 individual evolution times with a conventional mixing sequence that affects all spins in the sample

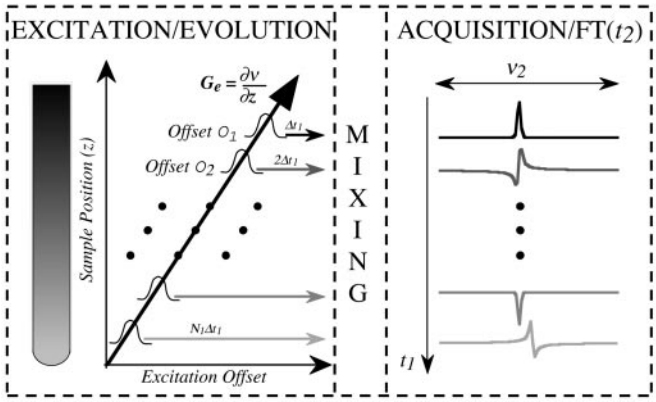

Fig. 2. Potential use of spectral heterogeneities toward the acquisition of multidimensional NMR data within a single scan. Heterogeneities are assumed to arise from the application of an external magnetic field gradient G_e. In combination with frequency-selective pulses, this enables spins throughout the sample to undergo spatially distinct t_1 evolution periods. Once spatially discriminated during the t_2 acquisition, this strategy allows one to collect a complete 2D NMR data set within a single scan.

simultaneously.[‖] A complete 2D NMR signal set can be retrieved from this encoded information if the spin evolution during t_2 is then collected in a spatially discriminated fashion. Of the several alternatives available for achieving such a goal with high resolution and within a single scan (23, 24), we assayed here the echo planar chemical-shift imaging technique. With it, the overall protocol succeeds in carrying out the acquisition of a complete 2D data set within one continuous signal scan while still relying entirely on FT principles.

The approach in Fig. 2 involves two imaging-type modules: one containing an initial spatially dependent evolution and another involving a final spatially discriminated detection. Both of these modules are achieved with the aid of external field gradients, the goal of which is to endow different locations within the sample with separate NMR frequencies. Yet the overall information being sought by the protocol as a whole is not spatial but spectroscopic. This in turn requires a complete refocusing of all spatially dependent spin precessions while leaving unaffected the intrinsic frequencies and correlations imparted by the spin Hamiltonians throughout the evolution, mixing, and acquisition periods. Of the several approaches that could be used to achieve such an objective, the one illustrated in Fig. 3 was used in this study. It consists of a train of inverting gradients $\pm G_e$ that enables the desired slice-selective initial excitation, and a final spatially resolved acquisition based on alternating $\pm G_a$ gradients. Because of their oscillatory nature, no cumulative effects are imparted by these gradients in either the t_1 or t_2 dimensions.

Results and Discussion

Fig. 4 illustrates further the potential of this scheme, with results obtained on a model organic sample using three homonuclear NMR experiments chosen for the distinct cross-peak patterns that they yield. These experiments include (*i*) a basic 2D sequence with an initial excitation pulse but no mixing event that only results in peaks along the main diagonal, (*ii*) a COSY sequence involving a $\pi/2$ mixing pulse meant to establish cross-peaks among directly J-coupled nuclei, and (*iii*) a TOCSY sequence that establishes cross-peaks via an isotropic mixing among all protons within a J-coupled network. The agreement

[‖]Similar effects could be achieved by applying a homogeneous excitation but spectrally selective mixing pulses or, in constant-time experiments, by using homogeneous excitation and mixing sequences but spectrally selective refocusing profiles. We find in certain cases some of these alternatives more convenient than that in Eq. **2**.

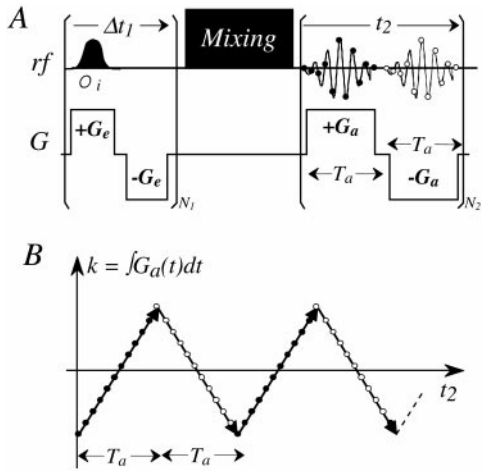

Fig. 3. (*A*) Generic scheme capable of affording 2D NMR spectra within a single scan. A train of frequency-shifted excitation pulses is applied in the presence of alternating field gradients to achieve an incremented evolution of spins throughout different positions in the sample (t_1); precession frequencies during the acquisition period then are monitored for each of these positions by using an EPI-type protocol (t_2). The nature of the mixing sequence is arbitrary. Throughout our experiments the B_o field heterogeneities were introduced along the main axis of a conventional sample tube by using the *z* gradients that are currently available in a majority of solution NMR systems. (*B*) EPI-type scanning of the mixed (k,t_2) acquisition space resulting from the pulse sequence shown in *A*. The dots symbolize points scanned during the course of positive and negative acquisition gradients; interleaved points then are sorted out as independent rows of two 2D data sets and processed individually (4, 23). Both 2D data sets can then be co-added for the sake of improving S/N by a $\sqrt{2}$ factor as was done for Fig. 1.

between the results afforded by these ultrafast 2D NMR experiments and their *a priori* expectations is excellent, an encouraging observation given the ample room available for further improving both the hardware as well as the pulse sequences supporting our acquisition principle.

An unusual feature of the approach that was just described is that it not only provides 2D NMR data sets within a single scan but may also do so without requiring the typical 2D numerical Fourier transformation involved in conventional acquisitions. Indeed the use of a slice-selective encoding during t_1 followed by a slice-selective decoding during t_2 amounts to a built-in FT along the indirect domain. This feature can be appreciated from the mathematical derivation of the signal arising from the schemes illustrated in Figs. 2 and 3. Because the physical collection of data during such an experiment is carried out while implementing a spatially resolved EPI-type acquisition, its resulting signal can be described as depending on two independent extraction variables: a time t_2 encoding spectral frequencies ν_2 during the acquisition time, and a variable $k = \int G_a(t)dt$ encoding the spatial positions z of spins within the sample. Considering as well that spins at different z positions were endowed with different t_1 evolution times, this signal can be summarized as

$$S(k, t_2) = \int_z \int_{\nu_2} \int_{\nu_1} [P(z, \nu_1, \nu_2) e^{i\nu_1 t_1(z)} e^{i\nu_2 t_2} e^{ikz}] d\nu_1 d\nu_2 dz. \quad [3]$$

Here $P(z, \nu_1, \nu_2)$ is the joint probability distribution that spins at a coordinate z will have precessed at a particular set of spectral frequencies ν_1 during t_1 and ν_2 during t_2. Assuming for simplicity static z slices that are being homogeneously excited leads to a joint spatial/spectral distribution $P(z, \nu_1, \nu_2) \approx \rho(z) \cdot I(\nu_1, \nu_2)$, where $I(\nu_1, \nu_2)$ is the 2D NMR spectrum being sought, and $\rho(z)$ is a shape function. For an ideal cylinder of constant composition this function will be simply a constant ρ. Fourier analysis along the k dimension then leads to

$$S(z, t_2) = \rho \int_{\nu_1} \int_{\nu_2} I(\nu_1, \nu_2) e^{i\nu_1 t_1(z)} e^{i\nu_2 t_2} d\nu_1 d\nu_2. \quad [4]$$

If it is now assumed that, as was actually done for acquiring the data, t_1 was incremented linearly with the z position of the spins, $t_1(z) = C \cdot (z - z_o)$, and it is clear that 2D FT of $S(z, t_2)$ will yield the desired $I(\nu_1, \nu_2)$ 2D NMR spectrum. Yet because the Fourier transformation is a self-reciprocal operation, it also follows that a second FT along the z dimension will simply revert the signal back into its original k-space distribution. A single 1D FT of the $S(k, t_2)$ data along t_2 is thus sufficient to retrieve the complete 2D $I(\nu_1, \nu_2)$ spectrum.

Equations aside, this explanation gives further physical insight into the origin and shape of peaks in this type of experiment. To appreciate this it is illustrative to consider the line shapes expected after subjecting a typical $S(k, t_2)$ imaging/spectroscopic signal to t_2 Fourier transformation: peaks will then be observed along ν_2 at the appropriate Ω_2 frequencies present in the sample, whereas sharp echoes centered at $k = 0$ and possessing point-spread functions proportional to $\int_z P(z) e^{ikz} dz$ will be encoded along the gradient k domain. If, however, spins have been

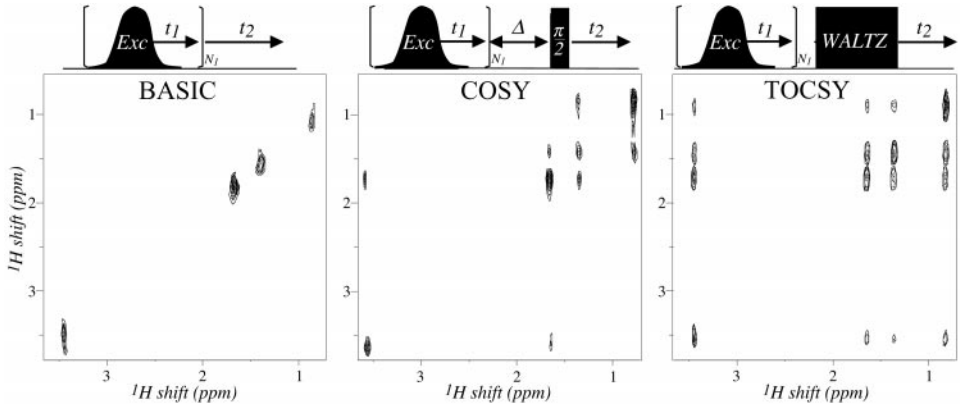

Fig. 4. Phase-sensitive single-scan 2D ^{1}H NMR spectra recorded within ≈0.22 s on a 20% (vol/vol) solution of *n*-butylchloride, $CH_3CH_2CH_2CH_2$-Cl, dissolved in $CDCl_3$. The pulse sequences used for acquiring these spectra are shown (*Upper*), with Δ set to 20 ms in the COSY and a 74-ms-long WALTZ sequence used for the TOCSY. Data were acquired with $N_1 = 40$ initial Gaussian pulses being applied at 4-kHz offset increments, while in the presence of $\gamma_H G_e = 150$ kHz/cm, and an acquisition involving 256 gradient echoes of the same magnitude with $T_a = 340$ μs long and 10-μs dwell times. All remaining pulses were applied nonselectively.

initially subject to an excitation of the type illustrated in Figs. 2 and 3 with $t_1(z) = C\cdot(z - z_o)$, an additional z-dependent dephasing proportional to $\Omega_1 t_1 = \Omega_1 \cdot C \cdot z$ will also become part of the total gradient encoding. After FT along t_2 signals will then be shifted from their original $k = 0$ positions to coordinates $(k, \nu_2) = (-C\cdot\Omega_1, \Omega_2)$, thus simultaneously defining both the Ω_1 and the Ω_2 frequencies for each chemical site.

These arguments also clarify the line shapes defining this type of 2D spectroscopy. Multidimensional peaks will be dictated here by the conventional *absorptive* + $i \cdot$ *dispersive* combination along the direct ν_2 domain, and by the FT of the sample's excited profile along the k-encoded axis. Assuming an ideal excitation of contiguous slices and the usual (rectangular) sample profile of conventional NMR tubes, real-only sinc-type point-spread functions thus emerge for the line shapes along the k axis. It follows that purely absorptive 2D peaks are an inherent feature of this acquisition mode. These arguments allow us as well to derive the Nyquist relations associated to this acquisition scheme. Sampling conditions along the ν_2 dimension will be as for a conventional EPI-shift experiment: denoting the length of the k-axis scan as T_a (Fig. 3), consecutive points along the t_2 axis will be spaced by $2T_a$ dwell times and result in $2N_2 \cdot T_a$ total t_2 acquisition times and $SW_2 = (2T_a)^{-1}$ spectral widths. Nyquist conditions along the ν_1 dimension will be dictated by a combination of the EPI acquisition parameters and the selective excitation conditions used for the initial encoding. Referring again to the simplest $t_1(z) = C\cdot(z - z_o)$ sequential excitation scheme, we conclude that under ideal conditions SW_1 will depend on the magnetogyric ratios γ_e and γ_a of the species being excited and detected, the gradient strengths G_e and G_a used to encode and decode positions during the excitation and acquisition, the $2T_a$ dwell time along t_2, the temporal delay Δt_1 between the initial excitation pulses, and the constant $\Delta O = |[O_{i+1} - O_i]|$ offset increment characterizing this pulse train. The resulting spectral span then can be summarized by $SW_1 = \Delta O \cdot [\gamma_a G_a T_a]/[\gamma_e G_e \Delta t_1]$, an expression of practical quantitative use for evaluating this type of experiments.

Also worth commenting on is the S/N expected for this type of experiments. From the slice-selective considerations in Fig. 2 one could assume that this class of experiments will be feasible only if, for a particular chemical site, each of the excited slices has enough S/N to afford a complete 2D NMR spectrum. This argument, however, would ignore that in the final scheme signals from all slices end up contributing to every (Ω_1, Ω_2) peak in the spectrum. One could also expect translational motions to count as important factors in attenuating these gradient-based experiments, yet the fact that gradient echoes are a feature of both the excitation and acquisition portions of the sequence alleviates considerably the potentially destructive effects of molecular diffusion. In fact it appears as if, except for potential dissipative processes occurring throughout the sequences (T_1 and T_2 relaxation, storage processes, etc.), the integrated signal intensity arising from diagonal and cross-peaks at a given Ω_2 frequency will be comparable, in principle, to the $I(\Omega_2)$ observed in a one-scan 1D spectrum. This does not mean, however, that the S/N observed throughout our measurements were as good as in their optimized 1D NMR counterparts. Some of these signal losses could be traced to nonidealities in the selective pulses and in the fast-switching gradients that were used. Yet even if these preventable losses were to be removed via further optimizations, a noise penalty would have to be paid for the sake of rapidly sampling both dimensions of the experiment in a single scan. Indeed if $\approx N_1$ points are to be collected during the course of each T_a gradient application, the filter width of the spectrometer needs to be opened to accommodate *ca.* N_1/T_a spectral widths. As a result there will be a noise increase of $\sqrt{2N_1}$ *vis-à-vis* the noise that would characterize a conventional 1D acquisition. Consequently, although capable of affording a 2D NMR spectrum within a single scan, the S/N per unit time of these ultrafast acquisition experiments will be lower in general than that of their conventional counterparts.** Because of the reliance of ultrafast 2D NMR on a fast digitization of the signal along both spectral axes, it is hard to envision routes by which this penalty could be avoided.

Conclusion

We conclude by remarking the convenience of introducing at the current stage of NMR's maturity a fully multiplexed format for the acquisition of multidimensional NMR spectra. Indeed developments in probehead and magnet technologies have increased NMR's sensitivity by almost an order of magnitude during the last decade (25), thus limiting the acquisition times of many multidimensional NMR experiments to signal digitization rather than to S/N considerations. Research areas where this bonus in signal could be combined with the advantages of single-scan 2D acquisitions include the structural analysis of rapidly changing dynamic systems (e.g., folding proteins, ref. 26), the characterization of analytes subject to flow (as in emerging chromatography-NMR techniques, ref. 27), the rapid survey of large numbers of chemicals such as those made available by new combinatorial chemistry techniques (28), and the speeding up of quantum-computing algorithms based on multidimensional NMR (29). Ultrafast methods could also be of importance for shortening up a variety of NMR experiments that demand high spectral dimensionalities. These experiments include structural elucidations of very large biopolymers, systems with complexities that will eventually require ≥4D NMR for achieving sufficient spectral resolution but at the same time are generally incapable of withstanding the long times hitherto associated with such acquisitions. They also include hybrid imaging/spectroscopy techniques where 2D ^{1}H-X spectral correlations are combined with spatial localization methods (30), *in vivo* experiments that are usually discouraged by their relatively long acquisition times. In fact, extending the scheme in Eq. **2** to shorten nD experimental times into those of $(n - 1)$D acquisitions is straightforward. But the opportunity also arises to reduce 3D and 4D NMR acquisitions to just a few signal scans via the proper use of multiple x-, y-, and z-gradient encodings. Progress along these various research avenues will be detailed elsewhere.

**One could envision certain scenarios, involving for instance nuclei with very long longitudinal relaxation times, where this might not be the case, yet these would be exceptions rather than the rule.

We are grateful to Professor M. Fridkin (Weizmann Institute of Science) for his gift of the hexapeptide sample. This work was supported by The Philip M. Klutznick Fund for Research.

1. Grant, D. M. & Harris, R. K., eds. (1996) *Encyclopedia of NMR* (Wiley, Chichester, U.K.).
2. Pople, J. A., Schneider, W. G. & Bernstein, H. J. (1959) *High Resolution Nuclear Magnetic Resonance* (McGraw–Hill, New York).
3. Cohen, M. S., ed. (1987) *Ann. N.Y. Acad. Sci.* **508,** 1–537.
4. Callaghan, P. T. (1991) *Principles of Nuclear Magnetic Resonance Microscopy* (Oxford Univ. Press, Oxford).
5. Schmidt-Rohr, K. & Spiess, H. W. (1994) *Multidimensional Solid-State NMR and Polymers* (Academic, London).
6. Cavanagh, J., Fairbrother, W. J., Palmer, A. G. & Skelton, N. J. (1996) *Protein NMR Spectroscopy: Principles and Practice* (Academic, San Diego).
7. Brown, M. A. & Semelka, R. C. (1999) *MRI: Basic Principles and Applications* (Wiley–Liss, New York).
8. Buxton, R. B. (2001) *An Introduction to Functional MRI: Principles and Techniques* (Cambridge Univ. Press, Cambridge).
9. Schweiger, A. & Jeschke, G. (2001) *Principles of Pulsed Electron Paramagnetic Resonance* (Oxford Univ. Press, Oxford).
10. Mukamel, S. (2000) *Annu. Rev. Phys. Chem* **51,** 691–729.

11. Ernst, R. R. & Anderson, W. A. (1966) *Rev. Sci. Instrum.* **37,** 93–102.
12. Jeener, J. (September 1971), International Ampere Summer School, Basko Polje, Yugoslavia; lecture notes published (1994) in *NMR and More in Honour of Anatole Abragam*, eds. Goldman, M. & Porneuf, M. (Les Editions de Physique, Les Ulis, France).
13. Aue, W. P., Bartholdi, E. & Ernst, R. R. (1976) *J. Chem. Phys.* **64,** 2229–2246.
14. Marshall, A. G. & Verdun, F. R. (1990) *Fourier Transforms in NMR, Optical, and Mass Spectrometry: A User's Handbook* (Elsevier, Amsterdam).
15. Ernst, R. R., Bodenhausen, G. & Wokaun, A. (1987) *Principles of Nuclear Magnetic Resonance in One and Two Dimensions* (Clarendon, Oxford).
16. Kessler, H., Gehrke, M. & Griesinger, C. (1988) *Angew. Chem. Int. Ed. Engl.* **27,** 490–536.
17. McKinstry, R. C. & Feinberg, D. A. (1998) *Science* **279,** 1965–1966.
18. Stehling, M. K., Turner, R. & Mansfield, P. (1991) *Science* **254,** 43–50.
19. Bax, A., Mehlkoff, A. F. & Smidt, J. (1980) *J. Magn. Reson.* **40,** 213–219.
20. Blumler, P., Jansen, J. & Blumich, B. (1994) *Solid State Nucl. Magn. Reson.* **3,** 237–240.
21. Frydman, L. & Peng, J. (1994) *Chem. Phys. Lett.* **220,** 371–377.
22. Braunschweiler, L. & Ernst, R. R. (1983) *J. Magn. Reson.* **53,** 521–528.
23. Mansfield, P. (1984) *Magn. Reson. Med.* **1,** 370–386.
24. Lowe, I. J. & Wysong, R. E. (1993) *J. Magn. Reson. B* **106,** 106–109.
25. Service, R. F. (1998) *Science* **279,** 1127–1128.
26. Dobson, C. M. & Hore, P. J. (1998) *Nat. Struct. Biol.* **5,** 504–507.
27. Liu, H. H., Felten, C., Xue, Q.F., Zhang, B.L., Jedrzejewski, P., Karger, B., Lacey, M. E., Subramanian, R., Olson, D. L., Webb, A. G. & Sweedler, J. V. (1999) *Chem. Rev.* **99,** 3133–3152.
28. Shuker, S. B., Hajduk, P. J., Meadows, R. P. & Fesik, S. W. (1996) *Science* **274,** 1531–1534.
29. Madi, Z. L., Bruschweiler, R. & Ernst, R. R. (1998) *J. Chem. Phys.* **109,** 10603–10611.
30. Thomas, M. A., Yue, K., Binesh, N., Davanzo, P., Kumar, A., Siegel, B., Frye, M., Curren, J., Lufkin, R., Martin, P. & Guze, B. (2001) *Magn. Reson. Med.* **46,** 58–67.